RM No. L8H24a
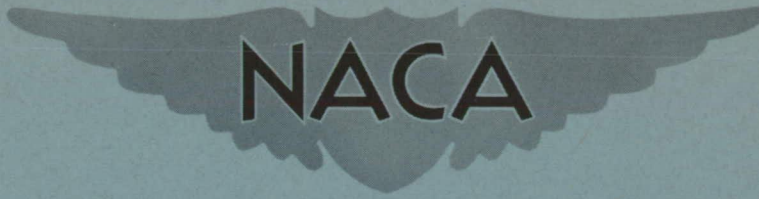
NACA

RESEARCH MEMORANDUM

CALCULATION OF THE EFFECTS OF STRUCTURAL FLEXIBILITY

ON LATERAL CONTROL OF WINGS OF ARBITRARY

PLAN FORM AND STIFFNESS

By

Franklin W. Diederich

Langley Aeronautical Laboratory
Langley Field, Va.

NATIONAL ADVISORY COMMITTEE
FOR AERONAUTICS
WASHINGTON

December 24, 1948

NATIONAL ADVISORY COMMITTEE FOR AERONAUTICS

RESEARCH MEMORANDUM

CALCULATION OF THE EFFECTS OF STRUCTURAL FLEXIBILITY

ON LATERAL CONTROL OF WINGS OF ARBITRARY

PLAN FORM AND STIFFNESS

By Franklin W. Diederich

SUMMARY

A method is presented for calculating the effectiveness and
reversal of lateral-control devices on wings of arbitrary plan form
and stiffness. Computing forms and an illustrative example are
included.

The margin against aileron reversal is shown to be relatively low
for swept wings at all speeds and for all configurations at supersonic
speeds; the margin is relatively high at subsonic speeds. Effectiveness
of conventional aileron configurations on sweptback wings at supersonic
speeds is relatively low.

INTRODUCTION

Adequate lateral control constitutes one of the more important
design requirements for airplanes. The ability of the airplane to
enter a roll is determined by the control power and is measured by the
maximum available rolling moment resulting from lateral-control deflection.
The degree of lateral maneuverability may be represented by the helix
angle at the wing tips corresponding to the highest rate of roll. The
lateral maneuverability depends both on the control power and the damping
in roll.

The control power and the damping in roll are affected by structural
flexibility. Control deflection ordinarily gives rise to aerodynamic
loads which tend to deform the wing structure in such a way as to reduce
the loads on it and thus to reduce the control power. If the dynamic
pressure of the air stream is sufficiently high, the amount of load
which results from the structural deformation may be sufficient to
nullify the effect of the control deflection. The speed and dynamic
pressure corresponding to this condition are known as the lateral-
control reversal speed or reversal dynamic pressure, since at a

2   NACA RM No. L8H24a

slightly higher dynamic pressure a control deflection in a given
direction would result in a rolling moment in a direction opposite
to that of the moment on a similar rigid wing.

Much of the early work on lateral-control reversal and loss of
control due to structural deformations was done in Great Britain. The
first published account of an investigation concerned with aileron
reversal appears to be reference 1. Even at that early date, aerodynamic
induction was taken into account, but an arbitrary wing-deflection mode
was assumed. The lateral-control power was analyzed on the basis of
the same assumptions in reference 2. The work done in Great Britain
subsequent to the publication of these two papers has been concerned
with more refined means of accounting for the actual stiffness
distributions and for aerodynamic induction; at the same time a great
deal of attention has been devoted to the simplification of the
numerical work required to obtain results in practical cases.

Work done on the problem of loss of lateral control due to wing
flexibility in this country (references 3, 4, and 5, for instance)
now represents the same stage of development as British work in the
field. Reference 3 presents convenient methods for determining the
aileron-reversal speed and other related critical speeds of wings of
arbitrary stiffness distribution; aerodynamic induction is taken into
account by means of an over-all correction. Reference 4 is concerned
with the determination of the lateral maneuverability and control
effectiveness. Aerodynamic induction is taken into account approxi-
mately, and the method is applicable to wings of arbitrary stiffness
distribution. The numerical work required for the analysis is
fairly extensive, however. Reference 5 shows a method for calculating
the reversal speed by matrix iteration; the method is convenient and
applicable to arbitrary stiffness distributions, but the integrating
matrices are only approximate and aerodynamic induction is taken into
account only by means of an over-all correction, unless suitable influence-
coefficient matrices are used in conjunction with the method.

.Although the foregoing methods and similar British work are
generally satisfactory for calculating the lateral-control effective-
ness and aileron-reversal speed of straight wings, they are inapplicable
to swept wings. The present paper is concerned with an analysis of
these problems for wings of arbitrary plan form, including swept plan
forms, as well as arbitrary stiffness. The method is based on the·
analysis of the loading of flexible wings presented in reference 6.
Since suitable aerodynamic-influence coefficients are not yet available,
aerodynamic induction is taken into account only as an over-all
correction and a slight reduction of the load at the tip, as in
reference 6. The method is formulated in such a manner, however, that
aerodynamic-influence coefficients may easily be included as soon as
they become available.

The numerical analysis required in any given practical case constitutes an extension of the calculations outlined in reference 6. Computing forms for the additional calculations required for an analysis of lateral-control effectiveness or reversal are presented in this paper. Their use is described in the section "Application of the Method." This section may be read without reference to the derivation of the method. As an example illustrating the method, the lateral-control effectiveness and reversal of the wing considered in reference 6 are analyzed in this paper. The reversal speeds of several wings derived from this wing by shifting the elastic axis and rotating the wing are calculated to demonstrate some general effects of sweep on the aileron-reversal speed.

SYMBOLS

The symbols used in the analysis are those of reference 6 with the following additions:

$[\bar{A}]$ auxiliary aeroelastic matrix

$[A_R]$ reversal matrix

cp_δ center of pressure of the load produced by aileron deflection, fraction of chord from leading edge

e_2 distance from the reference axis to the center of pressure of the load due to aileron deflection (positive rearward), fraction of chord

$[I_1]$ matrix defined in equation (11)

t distributed torque, inch-pounds per inch

y_i lateral ordinate of inboard end of aileron, inches

y_o lateral ordinate of outboard end of aileron, inches

α_δ angle of attack equivalent to unit aileron deflection

δ aileron deflection measured in planes parallel to the direction of flight, radians

ϵ moment-arm ratio $\left(\dfrac{e_2}{e_1}\right)$

DERIVATION OF THE METHOD

Assumptions

The assumptions made in the following analysis are the same as those made in reference 6. In addition it is assumed that the angle between the aileron and the wing is constant along the span of the aileron.

Air Loads

The aerodynamic forces on a wing section with control neutral are given in reference 6. In keeping with the aerodynamic assumptions the loading due to the aileron deflection is considered to be the corresponding strip loading multiplied by a reduction factor and rounded off at the tip. The effective section lift-curve slope appropriate to the aileron loading has approximately the same value as the effective slope appropriate to the linear-twist loading, as may be deduced by comparing the different J values presented in references 2 and 3.

The aerodynamic force on a wing section of unit width parallel to the direction of flight is then

$$l' = m_\theta q c \cos \Lambda \left(\alpha_s + \alpha_\delta \delta\right) \tag{1}$$

where α_δ is the aileron effectiveness factor $\left(\partial c_l/\partial\delta\right)\big/\left(\partial c_l/\partial\alpha\right)$. (See fig. 1.) The angle of aileron deflection δ is measured in planes parallel to the direction of flight. If it is desired to measure δ in planes perpendicular to some reference line, for instance, the quarter-chord line, the value of α_δ is replaced by a value α_{δ_Λ}, which is α_δ multiplied by the cosine of the sweep angle measured to the reference line. The moment of the running load about the elastic axis is

$$t' = m_\theta q e_1 c^2 \cos \Lambda \left(\alpha_s - \epsilon \alpha_\delta \delta\right) \tag{2}$$

where ϵ is the moment-arm ratio e_2/e_1 and $e_2 c$ is the distance between the center of pressure of the load due to aileron deflection and the reference axis. (See fig. 1.)

The accumulated torque and moment referred to the elastic axis may then be written as

$$\{T\} = m_\theta q s_\Lambda e_{1_r} c_r^2 \cos^3\Lambda [K_1]\left[\overset{o}{\dfrac{e_1}{e_{1_r}}\left(\dfrac{c}{c_r}\right)^2}\right]\left\{\{\alpha_s\} - \left[\overset{o}{\epsilon}\right]\{\alpha_\delta\delta\}\right\} \tag{3}$$

$$\{M\} = m_\theta q s_\Lambda{}^2 c_r \cos^2\Lambda\left\{\left[[K_2]\left[\overset{o}{\dfrac{c}{c_r}}\right] - \sin\Lambda\,\dfrac{e_{1_r}c_r}{s_\Lambda}\,[K_1]\left[\overset{o}{\dfrac{e_1}{e_{1_r}}\left(\dfrac{c}{c_r}\right)^2}\right]\right]\{\alpha_s\}\right.$$

$$\left. + \left[[K_2]\left[\overset{o}{\dfrac{c}{c_r}}\right] + \sin\Lambda\,\dfrac{e_{1_r}c_r}{s_\Lambda}\,[K_1]\left[\overset{o}{\dfrac{e_1}{e_{1_r}}\left(\dfrac{c}{c_r}\right)^2}\right]\left[\overset{o}{\epsilon}\right]\right]\{\alpha_\delta\delta\}\right\} \tag{4}$$

Equations of Equilibrium

The equations of equilibrium may be set up and treated in the same manner as in reference 6. The result is the relation

$$\{\alpha_s\} = a\left\{[A]\{\alpha_s\} - [\bar{A}]\{\alpha_\delta\delta\}\right\} \tag{5}$$

where a and $[A]$ are defined in reference 6, and the auxiliary aeroelastic matrix $\bar{A}$ is defined by

$$[\bar{A}] = \left[[K_3]\left[\overset{o}{\dfrac{(GJ)_r}{GJ}}\right] + \dfrac{(GJ)_r}{(EI)_r}\tan^2\Lambda\,[K_3]\left[\overset{o}{\dfrac{(EI)_r}{EI}}\right]\right.$$

$$\left. + \dfrac{w}{s_w}\left(Q_{\alpha_T} - \tan\Lambda\,Q_{\alpha_M}\right)[I_o]\right][K_1]\left[\overset{o}{\dfrac{e_1}{e_{1_r}}\left(\dfrac{c}{c_r}\right)^2}\right]\left[\overset{o}{\epsilon}\right]$$

$$+ \left[\dfrac{d}{a}[K_3]\left[\overset{o}{\dfrac{(EI)_r}{EI}}\right] - \dfrac{s_\Lambda}{e_{1_r}c_r\cos\Lambda}\,\dfrac{w}{s_w}\,Q_{\alpha_M}[I_o]\right][K_2]\left[\overset{o}{\dfrac{c}{c_r}}\right] \tag{6}$$

If structural influence coefficients of the type described in reference 6 are used instead of the stiffness curves, equation (5) takes the form

$$\{\alpha_s\} = a'\left\{[A']\{\alpha_s\}\quad [\overline{A}']\{\alpha_\delta\delta\}\right\} \tag{7}$$

where a' and $[A']$ are defined in reference 6 and

$$[\overline{A}'] = e_{1_r}c_r[\Phi_R][K_6]\left[\overset{o}{\frac{e_1}{e_{1_r}}\left(\frac{c}{c_r}\right)^2}\right]\left[\overset{o}{\epsilon}\right] - [\Phi_P][K_7]\left[\overset{o}{\frac{c}{c_r}}\right] \tag{8}$$

Solution of the Equations

The aerodynamic loading corresponding to a given aileron deflection may be obtained by writing equations (5) or (7) in the following form:

$$\left[[I] - a[A]\right]\{\alpha_s\} = - a[\overline{A}]\{\alpha_\delta\delta\} \tag{9}$$

Once the right-hand side of the equation (9) is multiplied out, the twist distribution $\{\alpha_s\}$ may be calculated by solving the simultaneous equations of equation (9). The loading as well as the accumulated torques and moments may be obtained from equations (1) to (4).

In order to calculate the aileron-reversal speed conveniently from equations (5) or (7), it is necessary to eliminate $\{\alpha_\delta\delta\}$ by expressing it in terms of $\{\alpha_s\}$. The required relation results from the condition that at the reversal speed the rolling moment vanishes, so that

$$\lfloor K_2\rfloor_1\left[\overset{o}{\frac{c}{c_r}}\right]\left\{\{\alpha_s\} + \{\alpha_\delta\delta\}\right\} = 0 \tag{10}$$

or

$$\lfloor K_2\rfloor_1\left[\overset{o}{\frac{c}{c_r}}\right]\{\alpha_\delta\delta\} = - \lfloor K_2\rfloor_1\left[\overset{o}{\frac{c}{c_r}}\right]\{\alpha_s\} \tag{10a}$$

where $\lfloor K_2 \rfloor_1$ is the first row of the $[K_2]$ matrix. The solution of equation (10a) may be shown to be (by the reasoning of reference 5)

$$\{\alpha_\delta\delta\} = - \frac{\left[\overset{o}{\alpha_\delta\delta}\right][I_1][K_2]\left[\overset{o}{\frac{c}{c_r}}\right]\{\alpha_s\}}{\lfloor K_2 \rfloor_1 \left[\overset{o}{\frac{c}{c_r}}\right]\{\alpha_\delta\delta\}} \tag{11}$$

where the matrix $[I_1]$ is defined by

$$[I_1] \equiv \begin{bmatrix} 1 & 0 & 0 & 0 & . & . \\ 1 & 0 & 0 & 0 & . & . \\ 1 & 0 & 0 & 0 & . & . \\ 1 & 0 & 0 & 0 & . & . \\ : & : & : & : & : & : \end{bmatrix} \tag{12}$$

If equation (11) is substituted in equation (5), the following relation is obtained:

$$\{\alpha_s\} = a\,[A_R]\{\alpha_s\} \tag{13}$$

where the aileron-reversal matrix $[A_R]$ is defined by

$$[A_R] = [A] + \frac{1}{\lfloor K_2 \rfloor_1 \left[\overset{o}{\frac{c}{c_r}}\right]\{\alpha_\delta\delta\}}\,[\bar{A}]\left[\overset{o}{\alpha_\delta\delta}\right][I_1][K_2]\left[\overset{o}{\frac{c}{c_r}}\right] \tag{14}$$

The reversal dynamic pressure is calculated by iterating equation (13) and substituting the critical value of a in the equation defining the parameter (equation (16) of reference 6).

APPLICATION OF THE METHOD

Selection of the Parameters

The section lift-curve slope and aerodynamic-center values are chosen for the Mach number of interest, as described in reference 6. At subsonic speeds the lift-curve slope is corrected for finite-span effects as described in said reference. Values of α_δ and cp_δ are best obtained from experimental section data at the appropriate Mach number. Theoretical thin-airfoil values of these parameters are presented in figure 1 for subsonic and supersonic speeds.

The structural parameters are obtained in the manner described in reference 6.

Calculation of Matrices

Either a 6-point or a 10-point solution may be employed. Computing forms are provided for the 6-point solution; similar forms may easily be set up for the 10-point solution.

In order to take account of the location of the inboard and outboard extremities of the aileron with the relatively few stations used in the analysis, equivalent δ values have to be used. These values are given in figure 2. They are intended to give a rounded off δ variation which has approximately the same area and the same moment about the root as the actual δ variation. The equivalent δ values of figure 2 pertain to actual values of δ equal to 1; they apply to ailerons which extend from y_1/s_w to the tip but can be combined to apply to any aileron configuration. Several examples are listed below for the six-point method, the actual values of δ being 1 and the equivalent

values being read from figure 2(a) as 0.716 for $\dfrac{y_i}{s_w} = 0.55$ and as

0.293 for $\dfrac{y_i}{s_w} = 0.95$:

Case	1	2	3	4	5
(y_i/s_w)	0.55	0.95	0.55	0	0
(y_o/s_w)	1.00	1.00	.95	1.00	.55
(y/s_w)	$\{\delta\}$				
0	0	0	0	1	1
.20	0	0	0	1	1
.40	0	0	0	1	1
.60	.716	0	.716	1	.284
.80	1	0	1	1	0
.90	1	.293	.707	1	0

(y_i/s_w) corresponds to the inboard
extremity of the aileron or elevon
(y_o/s_w) corresponds to the outboard
extremity of the aileron or elevon

The values for case 3 are obtained from those of cases 1 and 2, those
for case 5 from the ones of cases 1 and 4.

The $[A]$ matrix is calculated as described in reference 6. The
calculation of the auxiliary aeroelastic matrix then proceeds as shown
in table I; the numbering of the steps indicated in the upper left
corner of each block are a continuation of the steps in table VI(b)
of reference 6.

If it is desired to calculate the aileron-reversal dynamic pressure,
the aileron-reversal matrix is calculated by means of the form of table II.
The value of G is calculated by multiplying the first row of
matrix $[⑪]$ (see reference 6) by the column matrix $\{\alpha_\delta\delta\}$. In
accordance with equation (14), the $\{\alpha_\delta\delta\}$ values also occur as a diagonal
matrix; in this form they are divided by the G value and entered in
matrix $[⑯]$. The calculation then proceeds according to the
instructions of table II.

Special cases arise when any or all of the e_1 or e_2 values are zero. If only e_{1_r} is zero, the e_1 value at some other point may be used as a reference throughout the analysis and the parameter a redefined accordingly. The first column of the matrix $\left[\textcircled{14}\right]$ is calculated in this case by multiplying the first column of the matrix $\left[\textcircled{5}\right]\left[K_1\right]$ by the ratio $\dfrac{e_{2_r}}{e_{1_{ref.}}}$. Similarly, if some other e_1 value is zero, say the fourth along the span, e_{1_r} is used as a reference but the fourth column of $\left[\textcircled{14}\right]$ is calculated by multiplying the fourth column of the matrix $\left[\textcircled{5}\right]\left[K_1\right]$ by $\dfrac{e_{2_{(4)}}}{e_{1_r}}$, where $e_{2_{(4)}}$ is the value of e_2 at the fourth station, at which e_1 is zero.

If e_1 is zero along the entire span, some of the computing instructions given in this paper, as well as the ones given in reference 6, must be modified somewhat. In table VI(a) of reference 6 the $\left[\dfrac{e_2}{e_{2_r}}\left(\dfrac{c}{cr}\right)^2\right]$ matrix is entered in the space provided for the $\left[\dfrac{e_1}{e_{1_r}}\left(\dfrac{c}{cr}\right)^2\right]$ matrix. Some of the instructions of table VI(b) of reference 6 and table I of this paper are then modified as follows:

Step ⑥
$$\left[K_1\right]\left[\frac{e_2}{e_{2_r}}\left(\frac{c}{c_r}\right)^2\right]$$

Steps ⑧ to ⑬ as indicated for the case $e_1 = 0$ in reference 6.

Step ⑭
$$\frac{e_{2_r} c_r \cos \Lambda}{s_\Lambda} \frac{(EI)_r}{(GJ)_r} \frac{1}{\tan \Lambda} \left[\textcircled{7}\right]$$

All other instructions are unaffected.

If e_2 is zero along the span, table I of this paper may be modified as follows:.

Step ⑮
$$\left[\bar{A}\right] = \left[\textcircled{12}\right]$$

Step ⑭ may be omitted; all steps in table II are unaffected.

Calculation of the Aileron-Reversal Speed

The $[A_R]$ matrix is iterated in table III(a) to calculate the critical value of the parameter a and hence the critical speed. The calculation ordinarily has to be performed at least twice, once for subsonic speeds and once for supersonic speeds. From these critical values, from the definition of the parameter a, and from the effective lift-curve slope the dynamic pressure required for aileron reversal q_R may be calculated and plotted as a function of Mach number. If the actual dynamic pressure for the altitudes of interest is also plotted on the same chart, the lowest intersection of the reversal with a true-dynamic-pressure line will give the reversal Mach number and dynamic pressure at the altitude of the true-dynamic-pressure line.

The $[A_R]$ matrices calculated for the special cases mentioned in the preceding section do not all yield the critical value of the parameter a. When the value of e_1 is zero at the root, the critical value of the parameter a based on the reference value of e_1 will be obtained. If e_1 is zero at some other point along the span, or if e_2 is zero along the entire span, critical values of the parameter a will be obtained. In the case where e_1 is zero along the entire span, iteration of the A_R matrix calculated by following the instructions of the preceding section will yield the value of the parameter d at divergence.

In some of these special cases, and possibly in other cases as well, it may be found that the iteration procedure does not converge. In those cases the critical value of the parameter a (or d) is imaginary, so that there is no physical reversal speed and the wing under consideration is safe against reversal (in the speed range under consideration). If the critical value of the parameter a has the sign opposite to that of the value of e_{1_r} (or the other value of e_1 used as a reference) or if the critical value of d has the sign opposite to that of the sweep angle Λ, the reversal dynamic pressure will be negative. In that case also the wing is safe against reversal, since a negative reversal dynamic pressure cannot be obtained at any real speed.

Calculation of Control Power and Maneuverability

The calculation of the twist distribution for a given aileron deflection is carried out in table III(b). The matrix $\left[[I] - a[A]\right]$ is entered at the left and the column $\{\alpha_\delta \delta\}$ at the right. Usually

it will be convenient to let $\alpha_\delta \delta = 1$ (except where modified by fig. 2) and then multiply the resulting twist distribution and rolling power by the true $\alpha_\delta \delta$ values if desired. The $\{\alpha_\delta \delta\}$ column is then premultiplied by the $[\bar{A}]$ matrix (step ⑮ or ⑮ₐ) and entered in the second column at the right, which in turn is multiplied by $-a$ to yield the third column. The simultaneous equations with the coefficients at the left and the knowns at the right (the third column) are then solved for the unknown α_s values.

It will be noted that if the same values of a are selected as were used, in the calculation of the aerodynamic loading by the method of reference 6, the $\left[[I] - a[A] \right]$ matrix will already be available. If, in addition, Crout's method of solving simultaneous equations has been used to solve the simultaneous equations, the auxiliary matrix will also be available, so that calculation of the α_s values for the aileron loading will require very little time.

In some of the special cases discussed in the preceding sections care must be taken to use the proper parameters in conjunction with the matrices calculated for these special cases. In the case where e_{1_r} is zero, the a values must be based on the reference value of e_1 selected in calculating the matrix; in the case where e_1 is zero along the entire span the parameter d must be used instead of a in table III(b).

The resulting α_s values may be added to the effective $\alpha_\delta \delta$ values, multiplied by $\left(\dfrac{c_r}{\bar{c}} \right) \left[\dfrac{\delta}{c_r} \right]$, and plotted over the span to yield the aerodynamic load distribution $\left(\dfrac{cc_l}{\bar{c}m_e} \right)_{\alpha_\delta \delta = 1}$. The rolling-moment coefficient due to this forcing loading (over both wings) may be obtained from the relation

$$C_{l_w} = 2m_e \left(\frac{s_w c_r}{S/2} \right) \left(\frac{s_w}{2b} \right) \lfloor K_2 \rfloor_1 \left[\begin{matrix} 0 \\ \frac{\bar{c}}{c_r} \end{matrix} \right] \left\{ \{\alpha_s\} + \{\alpha_\delta \delta\} \right\} \qquad (15)$$

This coefficient, which is a direct measure of the rolling power, is seen to be dependent only on q/q_D (except for the factor m_e), since

$$\frac{q}{q_D} = \frac{a}{a_D}$$ and a_D is constant for a given speed range.

The rolling maneuverability depends not only on the rolling power but also on the damping in roll. The rate of roll per unit aileron deflection is given by

$$\left(\frac{pb}{2V}\right)_{\delta=1} = \alpha_\delta \frac{\left(C_{l_w}\right)_\delta}{\left(C_{l_w}\right)_p} \tag{16}$$

where $\left(C_{l_w}\right)_\delta$ is the forcing coefficient calculated from equation (15) with $\alpha_\delta \delta = 1$ and $\left(C_{l_w}\right)_p$ is the damping coefficient calculated from equation (40) of reference 6 for a value of $\alpha_g\left(= \frac{pb}{2V}\right) = 1$ at the wing tip.

Illustrative Example

The method described in the preceding sections has been used to analyze the lateral maneuverability of the wing considered in the illustrative example of reference 6. The required additional parameters of this wing are presented in table IV(a), which follows the form of table I. For convenience a value of $\alpha_\delta \delta = 1$ has been selected. The equivalent value of $\alpha_\delta \delta$ at the station $\frac{y}{s_w} = 0.4$ is obtained from figure 2 for the given values of y_i/s_w and y_o/s_w. The auxiliary elastic matrix for the subsonic case has been calculated by following the form of table I; the resulting matrix is shown in table IV(a).

The aileron-reversal matrix for the subsonic case is calculated by means of the form of table II. Several of the steps, as well as the result, are shown in table IV(b) for the subsonic case. Iteration of the aileron-reversal matrix (by means of the form of table III(a) or otherwise) yields a value of $a_R = 2.364$. A similar calculation for supersonic speeds yields a value of $a_R = 0.1280$. From these two values and the definition of the parameter a (see reference 6) the dynamic pressure required for reversal may be calculated and plotted against Mach number, as shown in figure 3. Also shown in figure 3 for comparison are the dynamic pressures required for divergence as well as the actual dynamic pressures at several altitudes. Where the dynamic pressure required for reversal is less than the actual dynamic pressure the aileron control is reversed. For the example wing reversal occurs at a Mach number of 1.3, approximately, at sea level.

The aerodynamic loading due to aileron deflection has been calculated by means of the form of table III(b). For the subsonic case and a value of $a = 0.552$ the $\left[[I] - a\,[A]\right]$ matrix is that shown in table X(b) of reference 6. The three columns at the right of table III(b) are given in table V. Also shown in table V are the values of the final matrix calculated from the third column, the values of $\dfrac{c_r}{\bar{c}}\left\{\dfrac{c}{c_r}\right\}$, the values of $\left\{\dfrac{cc_l}{\bar{c}m_\theta}\right\}_{\alpha_\delta\delta=1}$ for the twist distribution, which are obtained by multiplying the values of the preceding two columns by each other, and the values of $\left\{\dfrac{cc_l}{\bar{c}m_\theta}\right\}_{\alpha_\delta\delta=1}$ for the aileron-deflection distribution, which are obtained by multiplying the $\alpha_\delta\delta$ values by the $\dfrac{c_r}{\bar{c}}\left\{\dfrac{c}{c_r}\right\}$ values.

The aileron-deflected distribution given by the last column applies directly only to the rigid-wing case; it is plotted as such in figure 4. It will be noted that the equivalent $\alpha_\delta\delta$ value of figure 2 affords a convenient guide for fairing or rounding off the $\alpha_\delta\delta$ distribution. For the flexible wing the calculated twist distributions, such as the one shown in the next to the last column of table V, must be added algebraically to the aileron-deflected distribution. This is best done by first plotting them separately and then adding them point for point to the aileron distribution. The net distributions obtained in this manner for several cases are shown in figure 4. It is seen immediately that the distribution for case 5 $\left(\text{supersonic speeds,}\right.$ $\dfrac{q}{q_D} = -1.00\left.\right)$ indicates that the wing is operating at a speed above its reversal speed; actually the ratio q/q_R for this case is 1.154. The moments of the twist and aileron-deflected distributions are obtained by multiplying them by the first row of the K_2 matrix. The rolling-moment coefficient is obtained from equation (15) or by adding the moments of the aileron-distribution curve and the twist curve algebraically and multiplying the result by $2m_\theta\left(\dfrac{s_w\bar{c}}{S/2}\right)\left(\dfrac{s_w}{2b}\right)$. The ratio of the flexible-wing rolling-moment coefficient obtained in this manner to the corresponding rigid-wing rolling-moment coefficient is plotted in figure 5(a) against the ratio q/q_D. The lateral maneuverability is calculated by means of equation (16) using the damping coefficients calculated in reference 6 and is also plotted as a fraction of the rigid-wing value in figure 5(a). It will be noted that both the

maneuverability and the control power become zero at a value of $\frac{q}{q_D}$ = -0.87, which is indeed the ratio of the reversal to the divergence dynamic pressure at supersonic speeds, as is shown in figure 3.

Since the ratio q/q_D has been determined as a function of altitude and Mach number in figure 3 the parameters of figure 5(a) can be plotted as functions of altitude and Mach number, as has been done in figure 5(b). It is seen that the maneuverability and, to a lesser extent, the control power are relatively low at supersonic speeds, particularly at low altitudes. Since at high speeds even a small value of $pb/2V$ implies a fairly large value of the rate of roll p, this situation is not necessarily alarming. The wing in question should have adequate control at all speeds for altitudes greater than about 20,000 feet.

DISCUSSION

The discussion of the aerodynamic and structural assumptions of reference 6 is pertinent to the analysis of this paper as well. The additional aerodynamic assumption made in this paper, to the effect that aerodynamic induction effects may be estimated by reducing the strip-theory lift distribution by an over-all correction and rounding off the distribution both at the wing tip and at the aileron ends (using the equivalent values of fig. 2 as a guide), is consistent with the other aerodynamic assumptions. The reduction of the load distribution appears to be the same as that for a linear twist. A more refined way of taking the induction effects into account would be to use aerodynamic influence-coefficient matrices. As soon as suitable aerodynamic matrices become available they may be included in the method of this paper.

Two additional structural assumptions are made as well. In the first place, it is assumed that the angle δ between the wing and the aileron is constant along the span. This assumption appears to have been made in almost all of the published investigations into the problem of lateral-control reversal and appears to have yielded satisfactory results. The shorter the aileron and the greater the number of points at which the aileron is supported and at which its hinge moment is taken out the more nearly true the assumption would be.

In the second place, it is assumed that the control linkage is stiff, so that the aileron angle for a given stick displacement is independent of the dynamic pressure. This assumption need not be made if it is kept in mind that the results obtained by the method of this paper are for a given aileron angle and that the true aileron angle may be less at high dynamic pressures than at low ones. Thus, in order to account

for the control-linkage deflection, it is necessary only to calculate
the ratio of the true aileron angle at a given dynamic pressure to that
at zero dynamic pressure for the same stick position. The calculated
control moment and maneuverability must then be reduced by this factor.
Since deformations of the control linkage only affect the aileron
effectiveness, they have no bearing on the reversal speed. These
deformations may lead to aileron divergence for wings with heavily
overbalanced ailerons. This problem, as well as the problem of wing-
aileron divergence, has not been considered in the present analysis,
however.

The fuselage and tail do not contribute any appreciable amounts
to either the control or the damping moment, so that their effects may
ordinarily be neglected for the purpose of lateral-control calculations.
Similarly, the effect of wing camber does not enter into the problem
because the only important effect of camber is to give the flexible
wing a symmetrical lift distribution if it is set at the angle of
attack which would give zero lift for the rigid wing; this symmetrical
lift distribution has no effect on the lateral-control problem.

As in reference 6, the effects of the inertia loading on the
aerodynamic loading have not been considered explicitly in the analysis
of this paper. As pointed out in reference 6, however, the structural
deformations due to the inertia loading may be calculated conveniently
by means of the integrating matrices and then considered as part of
the geometrical angles of attack. This procedure may be applied in
the case of a rolling wing to determine the change in rolling moment
for a unit rolling acceleration at any given Mach number and dynamic
pressure. This rolling moment must be taken into account in estimating
the rolling accelerations due to a given forcing moment at any time
before the steady-roll condition is reached.

At transonic speeds there is considerable uncertainty in the
aerodynamic parameters. The control power is directly proportional
to the value of the parameter $c_{l_\delta} = m_0 \alpha_\delta$, which may be quite low
in the transonic region due to the fact that the aileron is located
in a region of separated flow. The method of this paper is applicable
to this case if the value of c_{l_δ} is known for the rigid wing. If
the decrease in this parameter due to flow separation is 40 percent
at a given Mach number and the loss in control power due to wing
flexibility amounts to 20 percent, for example, then the total loss
is 52 percent $(1 - 0.60 \times 0.80)$. The loss in maneuverability due to
the decrease in c_{l_δ} may be much less than the loss in control power,
however, since a decrease in c_{l_δ} would usually be accompanied by a
decrease in m_0, and hence in the damping coefficient.

Should the value of the parameter c_{l_δ} decrease to zero or reverse, aileron reversal will occur. This type of reversal is altogether different from the type of reversal discussed in this paper, since it is due entirely to aerodynamic action, whereas the reversal of concern in this paper is due to aeroelastic action. Both types of reversal are largely independent of each other; aerodynamic reversal will occur at a given speed regardless of the stiffness of the wing, whereas aeroelastic reversal will occur ordinarily at a different speed which is unaffected by the aerodynamic effectiveness.

As pointed out in reference 6, the method on which the analysis of this paper is based does not require the semirigid representation employed in many analyses of aerodynamic loading of flexible wings and of lateral-control reversal. The method of this paper takes the actual stiffness distribution and plan form into account; it integrates the differential equations exactly (within the accuracy of integrating matrices) without simplifying the wing to one of constant-chord segments with all the flexibility concentrated at the ends of the segments and without requiring time-consuming graphical integrations. Furthermore, the method of this paper furnishes the aerodynamic loading and hence the control power and maneuverability directly without iteration. An iteration is required to calculate the reversal speed, but this iteration is straightforward in application and converges rapidly in most practical cases. If it is preferred, the iteration may be dispensed with and the critical value of the parameter a determined

instead by setting the determinant of the matrix $\left[[I] - a[A]\right]$

equal to zero. This procedure implies calculating the coefficients of and solving a sixth-degree or tenth-degree equation in a (depending on whether the 6-point or the 10-point method is used), so that it is ordinarily more laborious than iterating the $[A_R]$ matrix.

Some general effects of sweep and of the moment arms e_1 and e_2 on the aeroelastic reversal speed may be of interest. The ratio of the reversal parameter a_R of a given wing to that of the unswept wing obtained by rotating the given wing a_{R_0} is shown in figure 6(a) plotted against a function of the sweep angle for subsonic and supersonic speeds; the two curves were obtained by considering the wing of the illustrative example to be rotated in such a manner as to keep the parameters $\dfrac{e_{1_r} c_r \cos \Lambda}{s_\Lambda}$, $\dfrac{(EI)_r}{(GJ)_r}$, as well as the chord, stiffness, and moment arm $(e_1$ and $e_2)$ distributions constant.

It appears that both sweepback and sweepforward tend to decrease the reversal parameter and hence the reversal speed. At supersonic

speeds, or more specifically, at small values of the parameter

$\dfrac{e_{2_r} c_r \cos \Lambda}{s_\Lambda} \sqrt{\dfrac{(EI)_r}{(GJ)_r}}$ the reversal speed for the sweptforward wing is

somewhat lower than that of the sweptback wing, whereas at higher
values of the parameter the variation of the reversal speed with the

sweep parameter $\tan \Lambda \sqrt{\dfrac{(GJ)_r}{(EI)_r}}$ is more nearly symmetrical with respect

to the zero-sweep case. There are some indications that this behavior
is not typical of all wings but rather is due to the fairly large
variations of the e_1 values, which also appear to be responsible for
the deviation from linearity of the $d - a$ curve of figure 7 of
reference 6, as well as of the e_2 and ϵ' values over the span of the
example wing. In general it appears that, for small values of the

moment-arm parameter $\dfrac{e_{2_r} c_r \cos \Lambda}{s_\Lambda} \sqrt{\dfrac{(EI)_r}{(GJ)_r}}$, the variation of the reversal

speed with the sweep parameter $\tan \sqrt{\dfrac{(GJ)_r}{(EI)_r}}$ should be nearly symmetrical

and that, for large values of the moment-arm parameter, the reversal
speed should tend to be lower for sweptback than for sweptforward wings.

The variation of the reversal speed of an unswept wing with the
moment-arm ratio is shown in figure 6(b) for wings which all have the
same distributions of the parameter e_1/e_{1_r} and e_2/e_{2_r} along the span

but have different values of e_{1_r} and e_{2_r}. The parameter a_{R_0} is

plotted against the ratio $\dfrac{1}{1+\epsilon}$, where the value of ϵ is selected

at the mid-aileron station. It is seen that the plot is linear for both
the subsonic and the supersonic case. The difference in these cases
is due to the different variation of e_1 and e_2 along the span; if
the variations were the same or if e_1 and e_2 were constant along
the span the two lines of figure 6(b) would coincide. Since the

reversal parameter a_{R_0} is proportional to $\dfrac{1}{1+\epsilon}$, and since the

reversal dynamic pressure is directly proportional to the reversal
parameter a and inversely proportional to the value e_{1_r} (by

definition of the parameter a), it follows that the reversal

dynamic pressure is approximately proportional to the ratio $\dfrac{1}{e_1 + e_2}$.

From figure 1 it is seen that the sum of e_1 and e_2 represents
the distance from the aerodynamic center to the center of pressure of

the lift due to aileron deflection and is independent of the location
of the elastic axis. This fact corroborates the commonly made
observation (see reference 1) that the reversal speed is independent
of the location of the elastic axis in the case of unswept wings.

The control power and maneuverability cannot be related to the
structural geometric parameters in as relatively simple a manner as the
reversal speed. The control power is a function of both the ratio q/q_R
and the ratio q_R/q_D; it normally decreases with q/q_R, the rate of
decrease being slow at first and then more rapid for positive values
of q_R/q_D (which would generally be obtained for unswept and sweptforward
wings) and vice versa for negative values of q_R/q_D (which would
generally be obtained for sweptback wings). The variation of the
maneuverability should generally be similar to that of the control
power, since the damping coefficient decreases (or in the case of
unswept and sweptforward wings increases) steadily with q/q_D and is
independent of q_R/q_D.

From the calculations for the example wings it appears that the
control power and maneuverability of sweptback wings tends to be relatively
low, particularly at supersonic speeds. If it should happen that a
combination of high sweep and large moment arm e_2 leads to an undesirably
low maneuverability and neither of these parameters can be changed, it
may be necessary to resort to unconventional control devices. Leading—edge
ailerons, for instance, have negative values of the moment arm e_2, so
that wings equipped with them tend to reverse at very high speeds, if at
all. This configuration has the additional advantage of relatively high
effectiveness at transonic speeds. On the other hand, the effectiveness
of leading—edge ailerons at subsonic speeds is so low that they would
have to be used in conjunction with trailing—edge ailerons if a great
deal of flying were to be done at subsonic speeds. Furthermore, they pose
a number of difficult structural and other design problems, so that it
would be well to consider them only as a last resort.

Another means of raising the reversal speed and of increasing the
control power is to change the stiffness of the structure. In general,
lateral control can be improved by increasing the torsional stiffness
or the bending stiffness. In some cases, however, the increase of the
reversal parameter due to a change in the parameter $\tan \Lambda \sqrt{\dfrac{(GJ)_r}{(EJ)_r}}$

(see fig. 6(a)) produced by a decrease in the torsional stiffness $(GJ)_r$
may be so rapid as to cause a net increase in the reversal speed. Finally,
any increase in the purely aerodynamic effectiveness α_δ of the aileron-
airfoil combination results in a proportional increase in the lateral
control effectiveness.

CONCLUDING REMARKS

A method has been presented for calculating the effectiveness and
reversal of lateral control as well as of the aerodynamic loading and
rolling moment produced by aileron deflection on flexible wings of
arbitrary plan form and stiffness.

It has been shown that the aileron-reversal speed decreases with
both sweepback and sweepforward and that the effectiveness of conven-
tional aileron configurations on sweptback wings at supersonic speeds
tends to be relatively low. The control effectiveness and the resulting
maneuverability of the airplane may be increased by varying the structural
stiffness and, if necessary, resorting to unconventional control devices,
such as leading-edge ailerons.

Langley Aeronautical Laboratory
      National Advisory Committee for Aeronautics
            Langley Field, Va.

REFERENCES

1. Pugsley, A. G.: The Aerodynamic Characteristics of a Semi-Rigid
      Wing Relevant to the Problem of Loss of Lateral Control Due to
      Wing Twisting. R. & M. No. 1490, British A.R.C., 1932.

2. Cox, H. Roxbee, and Pugsley, A. G.: Theory of Loss of Lateral
      Control Due to Wing Twisting. R. & M. No. 1506, British
      A.R.C., 1933.

3. Shornick, Louis H.: The Computation of the Critical Speeds of
      Aileron Reversal, Wing Torsional Divergence and Wing-Aileron
      Divergence. MR No. ENG-M-51/VF18, Addendum 1. Materiel Center,
      Army Air Forces, December 19, 1942.

4. Harmon, Sidney M.: Determination of the Effect of Wing Flexibility
      on Lateral Maneuverability and a Comparison of Calculated Rolling
      Effectiveness with Flight Results. NACA ARR No. 4A28, 1944.

5. Thomson, William T.: Aileron Reversal Speed by Influence
      Coefficients and Matrix Iteration. Jour. Aero. Sci., vol. 13,
      no. 4, April 1946, pp. 192-194.

6. Diederich, Franklin W.: Calculation of the Aerodynamic Loading of
      Flexible Wings of Arbitrary Plan Form and Stiffness. NACA RM
      No. L8G27a, 1948.

TABLE I. – CALCULATION OF THE AUXILIARY AEROELASTIC MATRIX

$$y_i/s_w \quad = \qquad\qquad y_o/s_w \quad =$$

$$\alpha_{\delta(SUBS)} = \qquad\qquad \alpha_{\delta(SUPERS)} =$$

$$CP_{\delta(SUBS)} = \qquad\qquad CP_{\delta(SUPERS)} =$$

y/s_w	$C_{\ell\,SUBS.}$	$C_{\ell\,SUPERS.}$	$\varepsilon_{SUBS.}$	$\varepsilon_{SUPERS.}$	δ or $\alpha_\delta \delta$
0					
.2					
.4					
.6					
.8					
.9					

η/s_a	$[\varepsilon]_{SUBS.}$
	0	.2	.4	.6	.8	.9
0		0	0	0	0	0
.2	0		0	0	0	0
.4	0	0		0	0	0
.6	0	0	0		0	0
.8	0	0	0	0		0
.9	0	0	0	0	0	

η/s_a	$[\varepsilon]_{SUPERS.}$
	0	.2	.4	.6	.8	.9
0		0	0	0	0	0
.2	0		0	0	0	0
.4	0	0		0	0	0
.6	0	0	0		0	0
.8	0	0	0	0		0
.9	0	0	0	0	0	

14 η/s_a	$[7][\varepsilon]_{SUBS.}$
	0	.2	.4	.6	.8	.9
0	0	0	0	0	0	0
.2						
.4						
.6						
.8						
.9						

14a η/s_a	$[7a][\varepsilon]_{SUPERS.}$
	0	.2	.4	.6	.8	.9
0	0	0	0	0	0	0
.2						
.4						
.6						
.8						
.9						

15 η/s_a	$[\bar{A}] = [12] + [14]$
	0	.2	.4	.6	.8	.9
0	0	0	0	0	0	0
.2						
.4						
.6						
.8						
.9						

15a η/s_a	$[\bar{A}] = [12a] + [14a]$
	0	.2	.4	.6	.8	.9
0	0	0	0	0	0	0
.2						
.4						
.6						
.8						
.9						

NACA

TABLE II.- CALCULATION OF AILERON REVERSAL MATRIX

First row of $[11]$:

$$G = \begin{array}{|c|c|c|c|c|c|} \hline 0 & & & & & \\ \hline \end{array} \{\alpha_\delta \delta\}$$

$$= \underline{\hspace{3cm}}$$

16	$\frac{1}{G}\left[\alpha_\delta^\circ \delta\right]$					
η/s_a	0	.2	.4	.6	.8	.9
0		0	0	0	0	0
.2	0		0	0	0	0
.4	0	0		0	0	0
.6	0	0	0		0	0
.8	0	0	0	0		0
.9	0	0	0	0	0	

	$[I_1]$					
η/s_a	0	.2	.4	.6	.8	.9
0	1	0	0	0	0	0
.2	1	0	0	0	0	0
.4	1	0	0	0	0	0
.6	1	0	0	0	0	0
.8	1	0	0	0	0	0
.9	1	0	0	0	0	0

17	$[16][I_1]$					
η/s_a	0	.2	.4	.6	.8	.9
0		0	0	0	0	0
.2		0	0	0	0	0
.4		0	0	0	0	0
.6		0	0	0	0	0
.8		0	0	0	0	0
.9		0	0	0	0	0

18	$[7][11]$					
η/s_a	0	.2	.4	.6	.8	.9
0	0					
.2	0					
.4	0					
.6	0					
.8	0					
.9	0					

SUBSONIC

19	$[15][8]$					
η/s_a	0	.2	.4	.6	.8	.9
0	0	0	0	0	0	0
.2	0					
.4	0					
.6	0					
.8	0					
.9	0					

SUPERSONIC

19a	$[15a][8]$					
η/s_a	0	.2	.4	.6	.8	.9
0	0	0	0	0	0	0
.2	0					
.4	0					
.6	0					
.8	0					
.9	0					

20	$[A_R]=[13]+[19]$					
η/s_a	0	.2	.4	.6	.8	.9
0	0	0	0	0	0	0
.2						
.4						
.6						
.8						
.9						

20a	$[A_R]=[13a]+[19a]$					
η/s_a	0	.2	.4	.6	.8	.9
0	0	0	0	0	0	0
.2						
.4						
.6						
.8						
.9						

NACA

Table III – Form for Solution of Aeroelastic Equation

(a) Reversal

(b) Twist due to Aileron Deflection

$\%_{b} = $ $\%_{R} = $ $a = $

$[I] - a[A]$

$[A_R]$

$\{\alpha_s\}$

$[A_R]\{\alpha_s\}$

Auxiliary matrix

Aux. matrix

Final matrix

$a_R = $

	① $\{\alpha_s \delta\}$	② $[A]\times$①	③ $-a\times$②

Table with entries including 1.0000, .3000, .5000, .7000, .9000, 1.0000 and column headers (1)(2)(3)(4)(5)(6), rows 0 .2 .4 .6 .8 .9.

TABLE IV- CALCULATION FOR THE EXAMPLE WING AT SUBSONIC SPEED

(a)- Auxiliary Aerodynamic Matrix

$y_1/s_w = .434$ $y_y/s_w = 1.000$

$\alpha_{\delta(subs)} = .547$ $\alpha_{\delta(supers)} = .20$

$CP_{\delta(subs)} = .458$ $CP_{\delta(supers)} = .90$

y/s_w	e_2 (SUBS)	e_2 (SUPERS)	ε (SUBS)	ε (SUPERS)	α_δ
0	.0058	.4478	.0287	16.46	0
.2	.0087	.4507	.0437	18.55	0
4	.0111	.4531	.0563	20.69	0.265
.6	.0136	.4556	.0701	23.48	1.000
.8	.0160	.4580	.0833	26.94	1.000
.9	.0173	.4593	.0906	29.25	1.000

$[\varepsilon]$ SUBS.	0	.2	4	.6	.8	.9
0	.0287	0	0	0	0	0
.2	0	.0437	0	0	0	0
4	0	0	.0563	0	0	0
.6	0	0	0	.0701	0	0
.8	0	0	0	0	.0833	0
.9	0	0	0	0	0	.0906

15 — $[\bar{A}] = [12a]+[14a]$	0	.2	4	.6	.8	.9
0	0	0	0	0	0	0
.2	-.00217	.01184	.02541	.08337	.03542	.06348
4	-.00433	.01706	.04563	.21248	.09066	.18577
.6	-.00433	.01706	.04041	.29601	.17065	.34430
.8	-.00433	.01706	.03443	.31802	.20199	.49812
.9	-.00433	.01706	.03443	.31802	.19534	.54309

(b)- Aileron Reversal Matrix

First row of $[10]$:

$$G = \left[\;0\;\;|\;.04826\;|\;.04925\;|\;.11456\;|\;.04549\;|\;.07917\;\right]\{\alpha_\delta\}$$

$$= 0.2507$$

16 — $\frac{1}{G}[\alpha_\delta]$	0	.2	4	.6	.8	.9
0	0	0	0	0	0	0
.2	0	0	0	0	0	0
4	0	0	1.05712	0	0	0
.6	0	0	0	3.98915	0	0
.8	0	0	0	0	3.98915	0
.9	0	0	0	0	0	3.98915

19 — $[5][18]$	0	.2	4	.6	.8	.9
0	0	0	0	0	0	0
.2	0	.02639	.02261	.08637	.03430	.05969
4	0	.09819	.08799	.23307	.09255	.16107
.6	0	.15819	.14176	.37550	.14911	.25950
8	0	.19777	.17723	.46945	.18642	.32443
.9	0	.20514	.18384	.48697	.19337	.33653

18 — $[17][10]$	0	2	4	.6	.8	.9
0	0	0	0	0	0	0
.2	0	0	0	0	0	0
4	0	.05102	.04572	.12110	.04809	.08369
.6	0	.19252	.17253	.45700	.18147	.31582
.8	0	.19252	.17253	.45700	.18147	.31582
.9	0	.19252	.17253	.45700	.18147	.31582

20 — $[A_R] = [13]+[19]$	0	.2	4	.6	.8	.9
0	0	0	0	0	0	0
.2	-.00414	.04310	.02545	.02357	.00433	.00372
4	-.00774	.12000	.09385	.10715	.01583	.00695
.6	-.00774	.18000	.15503	.26327	.04642	-.00732
.8	-.00774	.21958	.18440	.38811	.10027	.00400
.9	-.00774	.22695	.19101	.40563	.10911	.04635

NACA

TABLE V - CALCULATION OF AERODYNAMIC LOADING FOR EXAMPLE WING

$a = .552$

η/s_a	① $\{\alpha_\delta\ \delta_f\}$	② $[A]\cdot\{\theta\}$	③ $-a\times\{②\}$ Final matrix	$\frac{c_r}{\bar{c}}\{\frac{\bar{c}}{c_r}\}$	$\{\frac{c c_l}{\bar{c}\ m_e}\}^{(1)}_{\alpha_\delta,\delta_f=1}$	$\{\frac{c c_l}{\bar{c}\ m_e}\}^{(2)}_{\delta_f=1}$
0	0	0	0	1.266	0	0
.2	0	0.1890	-0.1043	-0.0699	1.145	-0.080
.4	0.265	0.5100	-0.2815	-0.1999	1.026	-0.205
.6	1	0.8217	-0.4536	-0.3392	0.906	-0.307
.8	1	1.0273	-0.5671	-0.4477	0.787	-0.352
.9	1	1.0656	-0.5882	-0.4773	0.726	-0.347

$\frac{c_r}{\bar{c}}\{\frac{\bar{c}}{c_r}\}$	$\{\frac{c c_l}{\bar{c}\ m_e}\}^{(1)}$	$\{\frac{c c_l}{\bar{c}\ m_e}\}^{(2)}$
1.266	0	0
1.145	-0.080	0
1.026	-0.205	0.272
0.906	-0.307	0.906
0.787	-0.352	0.787
0.726	-0.347	0.726

(1)- Twist distribution
(2)- Aileron- deflected distribution

$$\lfloor K_2 \rfloor, \left\{\frac{c c_l}{\bar{c}\ m_e}\right\}^{(1)}_{\alpha_\delta,\delta=1} = -0.138$$

$$\lfloor K_2 \rfloor, \left\{\frac{c c_l}{\bar{c}\ m_e}\right\}^{(2)}_{\alpha_\delta,\delta=1} = 0.317$$
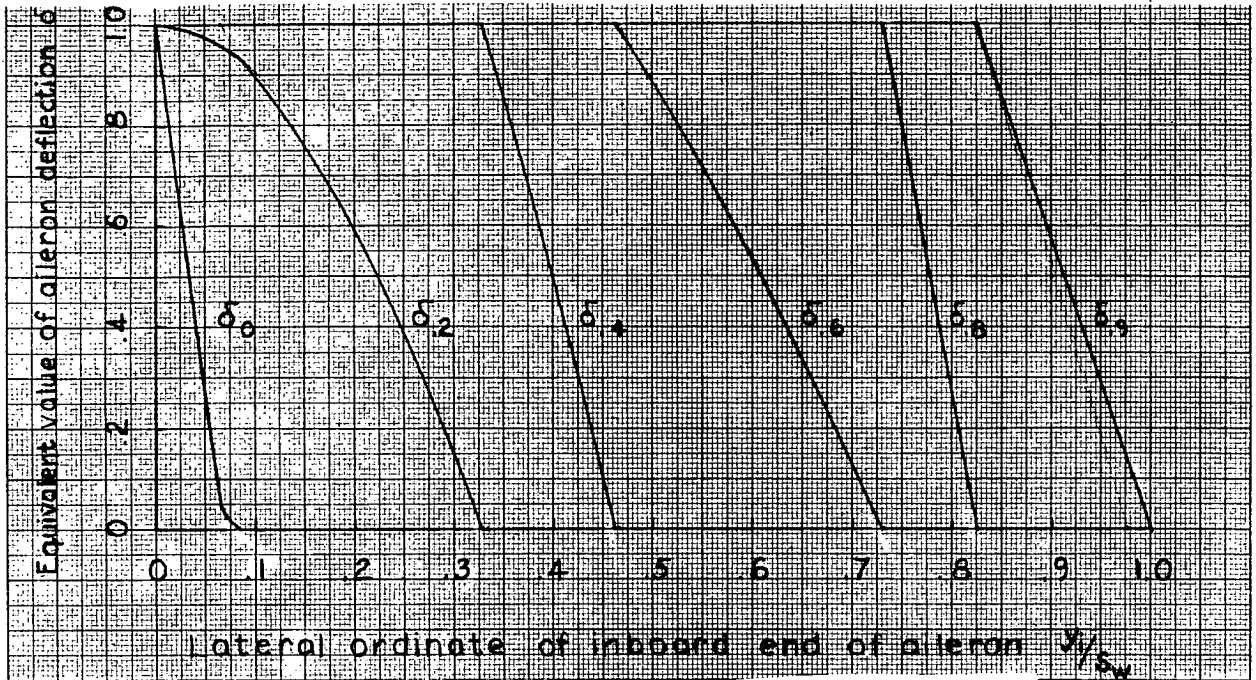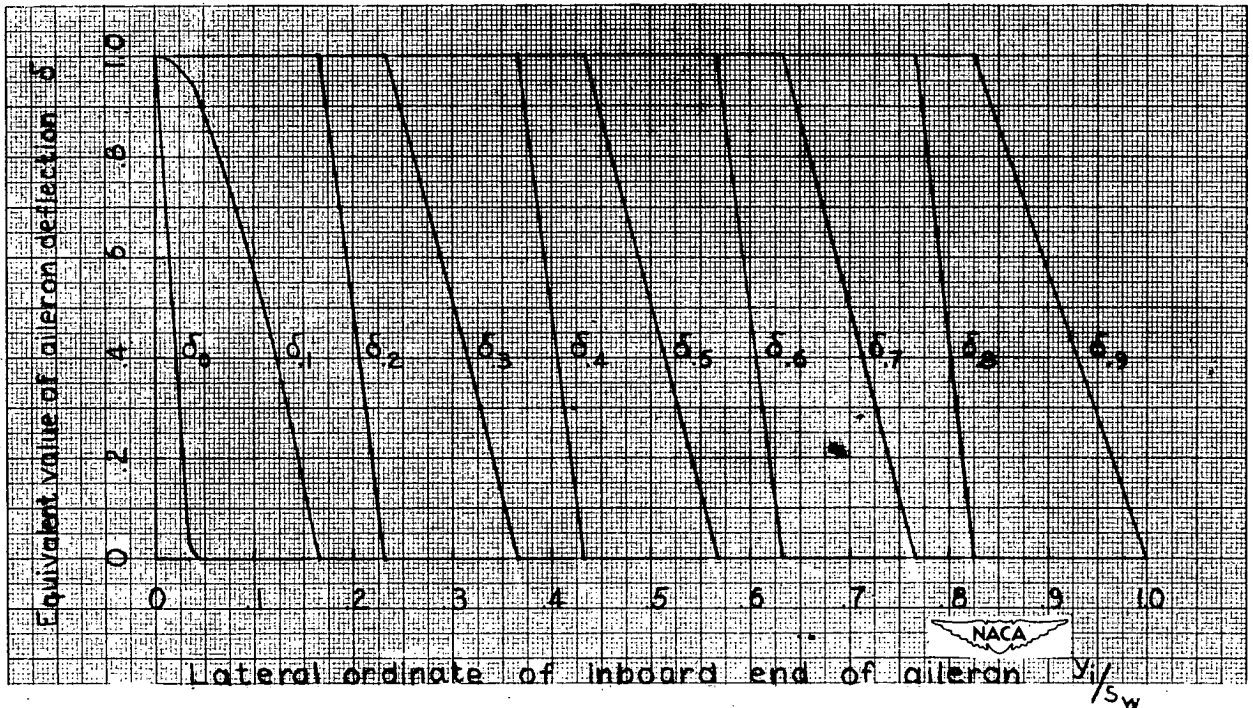
NACA
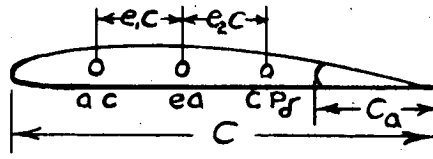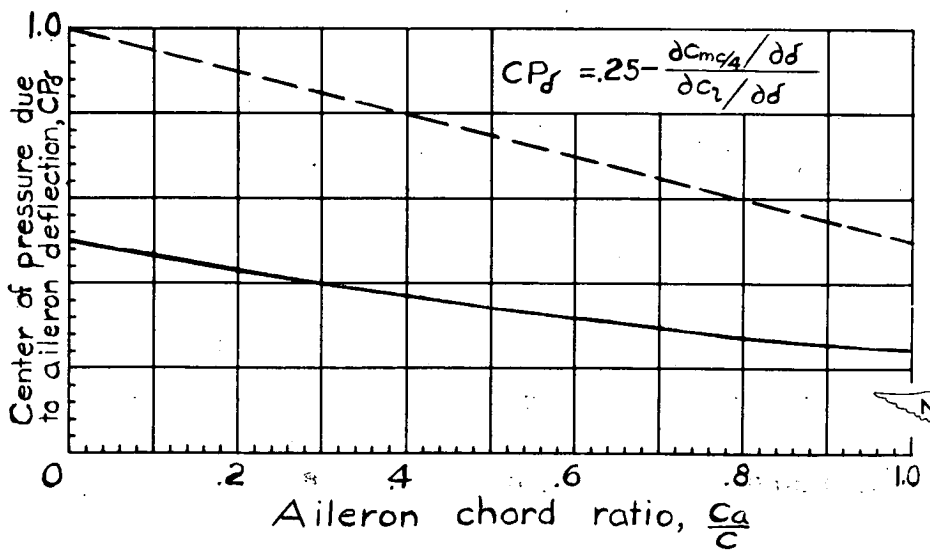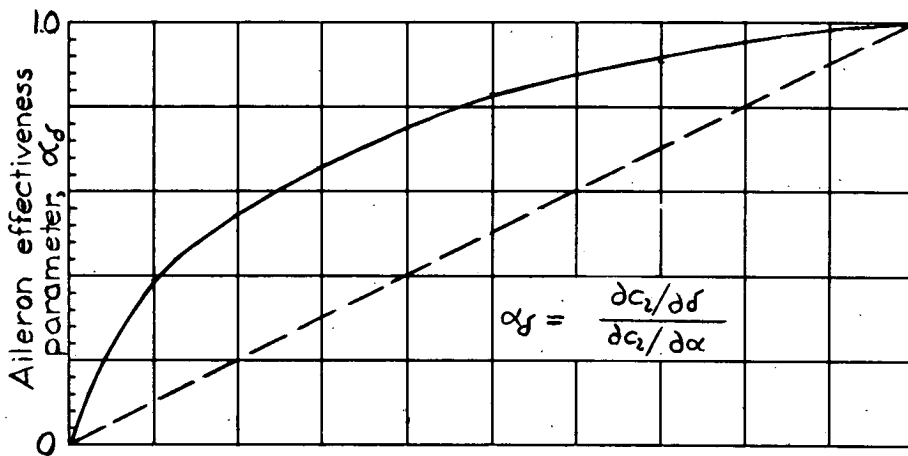
Figure 1.-   Definitions and theoretical values of the aileron force parameters.

(a) Six-point method.

(b) Ten-point method.

Figure 2.- Equivalent values of aileron deflection for unit actual deflection.
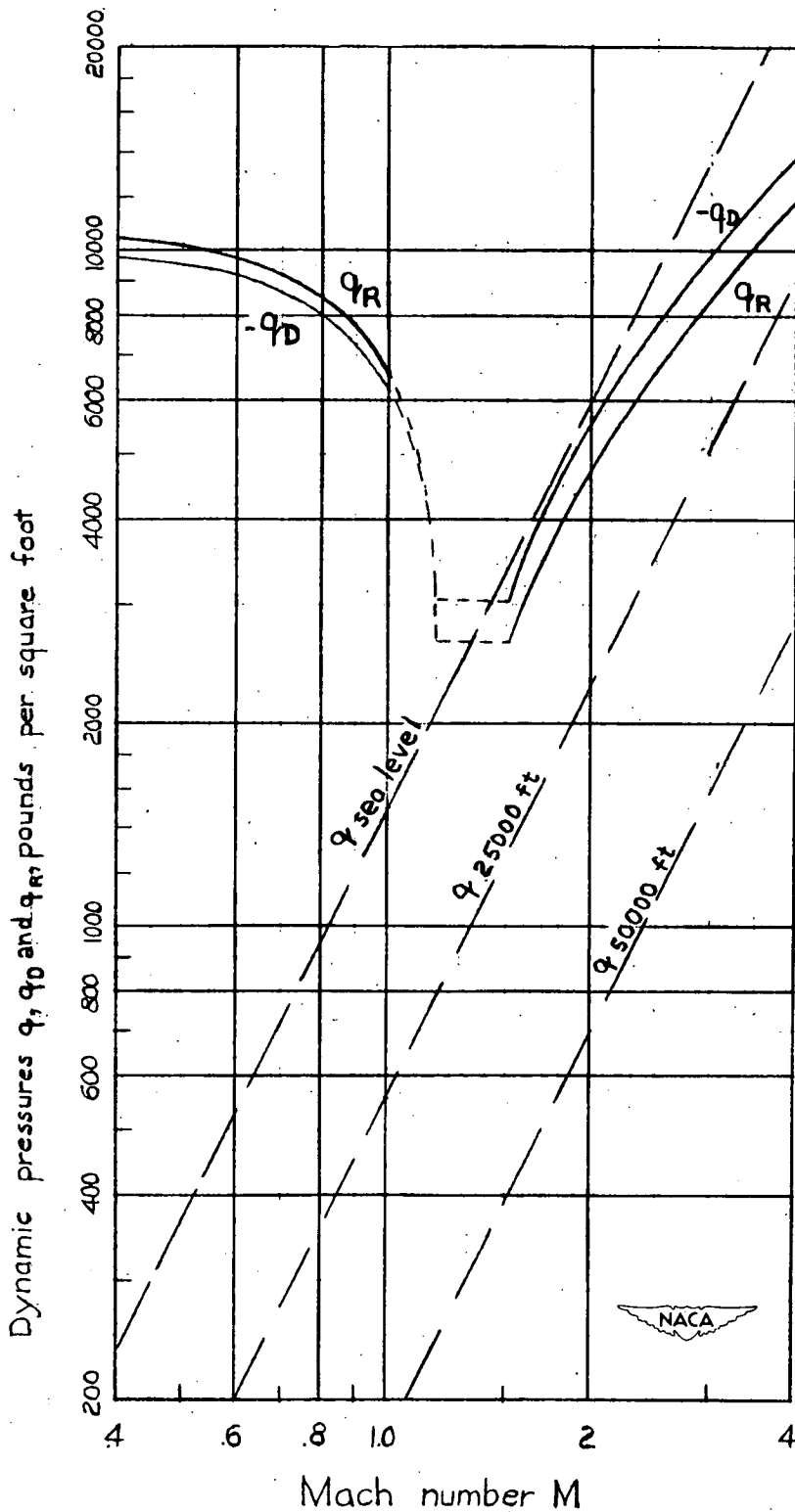
Figure 3.- Effect of Mach number on the critical and the actual dynamic
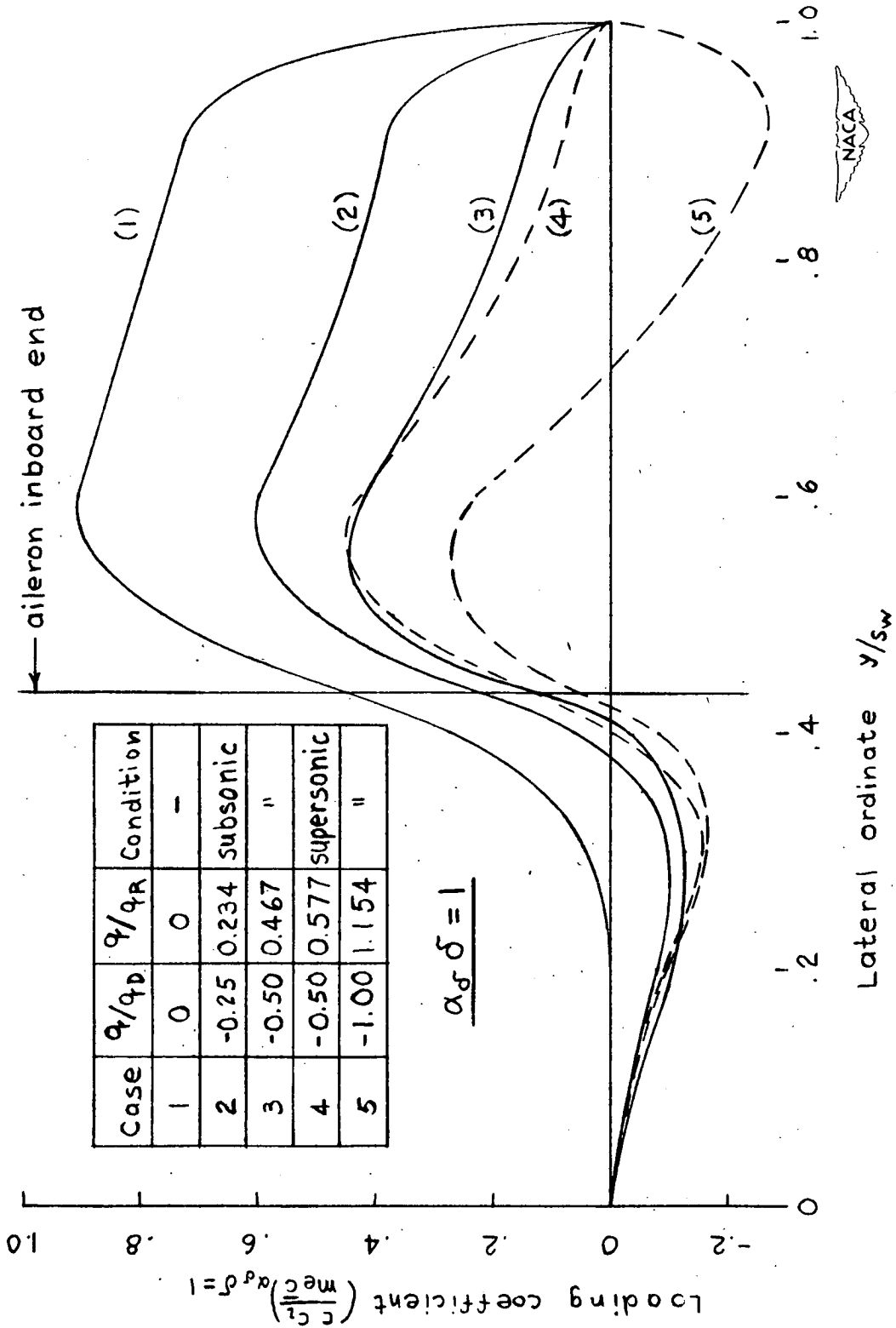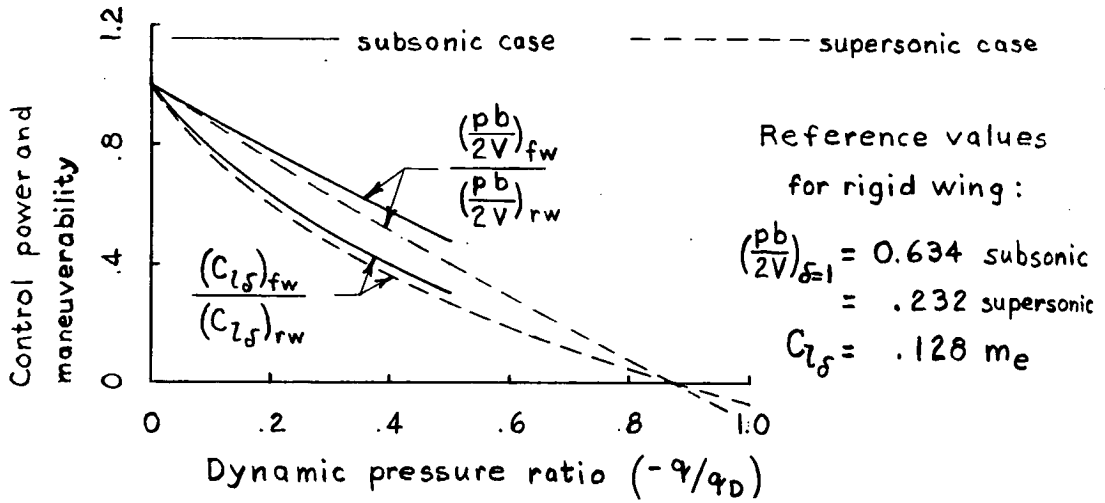pressures of the example wing.

Case	q/q_D	q/q_R	Condition
1	0	0	――
2	-0.25	0.234	subsonic
3	-0.50	0.467	"
4	-0.50	0.577	supersonic
5	-1.00	1.154	"

$$\alpha_d \, \delta = 1$$

Figure 4.- Loading of example wing with aileron deflected.
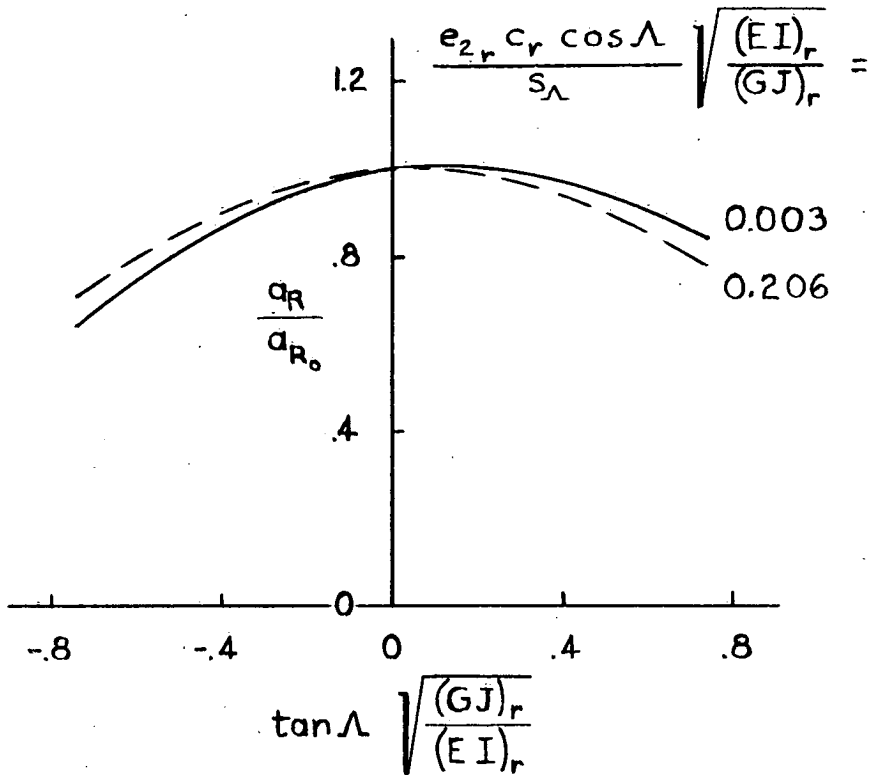
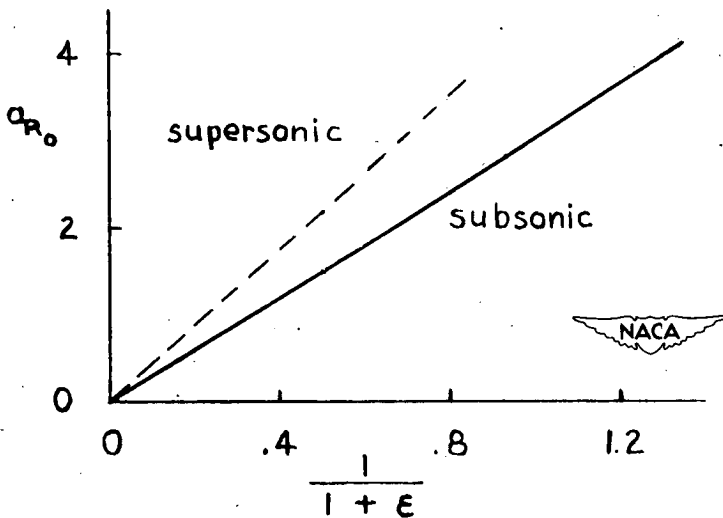(a) Variation with dynamic pressure ratio.
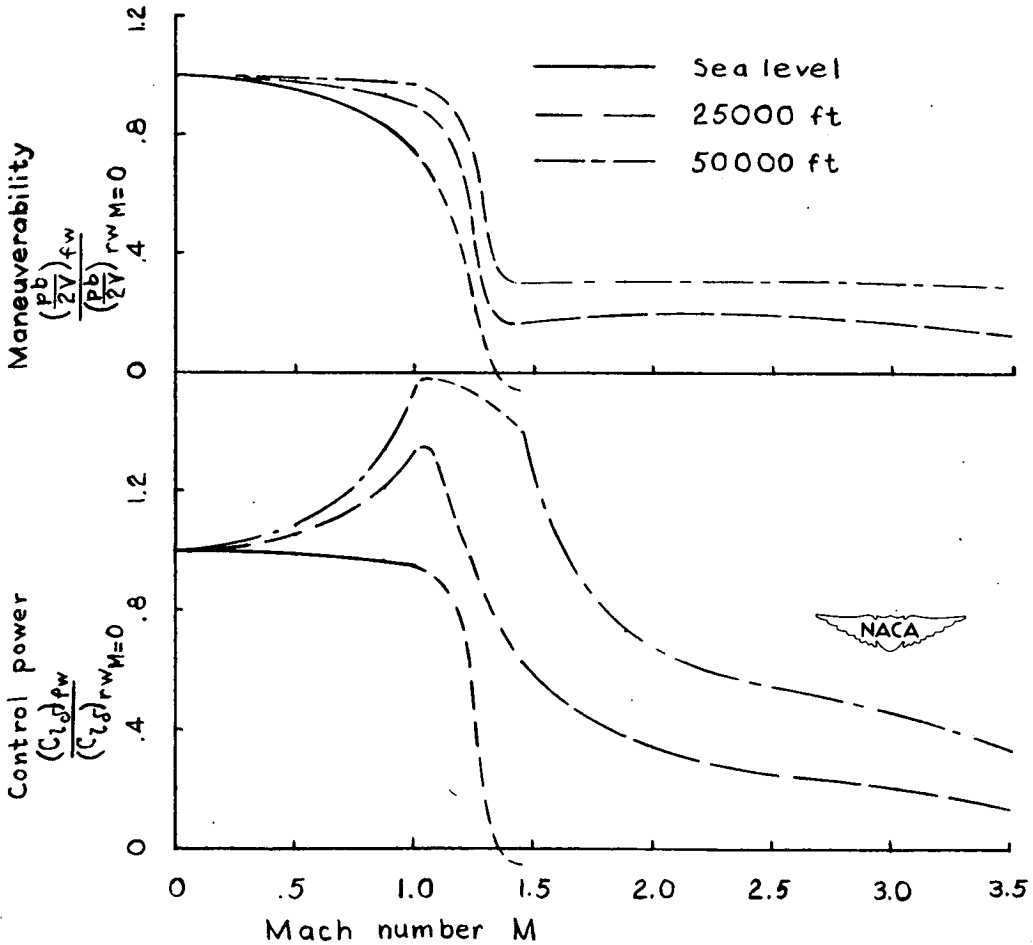
(b) Variation with Mach number and altitude.

Figure 5.- Control power and effectiveness of example wing.

(a) Effect of sweep on reversal parameter a_R.

(b) Effect of moment-arm ratio ϵ on reversal parameter a_{R_0} for unswept wings.

Figure 6.-   Effects of sweep and moment-arm ratio on reversal speed.